

## Truncation of CDK5 Activator p35 Induces Intensive Phosphorylation of Ser<sup>202</sup>/Thr<sup>205</sup> of Human Tau\*

Received for publication, July 24, 2002, and in revised form, September 9, 2002  
Published, JBC Papers in Press, September 10, 2002, DOI 10.1074/jbc.M207426200

Mitsuko Hashiguchi‡§, Taro Saito¶, Shin-ichi Hisanaga¶, and Toshio Hashiguchi‡

From the ‡Department of Physiology, Tokyo Medical University, 6-1-1 Shinjuku, Shinjuku, Tokyo 160-8402, Japan and the ¶Department of Biological Sciences, Graduate School of Science, Tokyo Metropolitan University, 1-1 Minami-ohsawa, Hachioji, Tokyo 192-0397, Japan

Hyperphosphorylated tau is a major component of neurofibrillary tangles, one of the hallmarks of Alzheimer's disease. CDK5 is a kinase that phosphorylates the tau protein, and its endogenous activator, p35, regulates its activity. Recently, calpain was found to digest p35 to its truncated product, p25. Several lines of evidence suggest that p25-CDK5 has much more powerful kinase activity and that it may cause abnormal hyperphosphorylation of tau. In this study, we have examined the kinetic characteristics of *in vitro* phosphorylation of the longest isoform of human tau by CDK5 and its activators using recombinant proteins. Although the kinase activity of CDK5 in phosphorylating tau was significantly higher in the presence of p25, the affinity of CDK5 for tau was not different. Phosphopeptide mapping revealed enhanced phosphorylation of Ser<sup>202</sup>/Thr<sup>205</sup> residues by p25-CDK5 (amino acid residues of tau are numbered according to the longest isoform of human tau). These results suggest that cleavage of p35 to p25 greatly enhances the kinase activity of CDK5 and increases the phosphorylation of Ser<sup>202</sup>/Thr<sup>205</sup>. Considering the fact that phosphorylation of Ser<sup>202</sup>/Thr<sup>205</sup> antagonizes the tau-mediated nucleation of tubulin, p25-CDK5 may play a pivotal role in neuronal cell death in Alzheimer's disease.

Aberrant phosphorylation of the tau protein is considered to play a decisive role in the pathogenesis of neurodegenerative disorders collectively called tauopathies (1). Tau is a neuron-specific, microtubule-associated protein that plays major roles in the assembly and stabilization of microtubules. In the brains of patients with Alzheimer's disease, abnormally phosphorylated tau protein, paired helical filament (PHF)<sup>1</sup> tau, becomes dissociated from neuronal microtubules and accumulates in PHFs, the filamentous network generated by self-aggregation of hyperphosphorylated forms of tau. All six adult isoforms of tau are known to be hyperphosphorylated in PHFs (2).

Several lines of evidence suggest that proline-directed serine/threonine kinases, together with protein phosphatases, play an important role in the hyperphosphorylation of tau (3). Candidate protein kinases include mitogen-activated protein kinase, glycogen synthase kinase-3 $\beta$ , and cyclin-dependent ki-

nase-5 (CDK5). None of these enzymes can generate PHF-tau alone (4).

CDK5, initially known as brain proline-directed protein kinase or neuronal cdc2-like protein kinase, phosphorylates tau at a high stoichiometry (5, 6). Unlike other tau kinases, the activity of CDK5 is regulated by endogenous regulatory proteins, p35 and p39. In this respect, CDK5 is distinctly different from other tau kinases (7).

Recently, calpain, a calcium-dependent protease, was found to digest both p35 and p39 to their truncated products, p25 and p29, respectively (8, 9). Furthermore, truncation of p35 to p25 and the subsequent formation of the p25-CDK5 complex result in neuronal cell death and hyperphosphorylation of tau (10). From these findings, the following hypothesis emerged. Initially, various stress signals activate calpain by recruiting intracellular Ca<sup>2+</sup>, and then the activated calpain digests p35 to p25. Finally, the p25-CDK5 complex hyperphosphorylates tau proteins, causing disruption of microtubule integrity and inevitable cell death (11).

Several criticisms of this hypothesis have appeared. Among them, the observed accumulation of p25 in the brains of patients with Alzheimer's disease may be accounted for by post-mortem degradation of p35 (12). In fact, p35 is notoriously unstable. Most brain-derived p35 is lost or truncated to p25 during purification. Thus, the kinetic activity of tau phosphorylation by p35-CDK5 is only poorly understood.

Lack of knowledge about the regulation of CDK5 by its activators, p35 and p25, severely limits our understanding of the possible pathogenesis induced by CDK5. We have examined the kinetic characteristics of *in vitro* phosphorylation of the longest isoform of human tau by CDK5 using recombinant proteins. This study clarified not only the kinetics of overall phosphorylation, but also the details of site-specific phosphorylation of human tau by CDK5 complexes.

### EXPERIMENTAL PROCEDURES

**Purification of Human Recombinant Tau**—Bacterially expressed tau, the longest isoform of human tau protein, was purified as described previously (13) with minor modifications. After addition of NaCl to 0.5 M, the bacterial extract was boiled in a hot bath for 10 min and centrifuged at 8000  $\times$  g. After dialysis in extraction buffer A (50 mM PIPES, pH 6.8, 1 mM EDTA, 1 mM dithiothreitol, and 0.2 mM phenylmethylsulfonyl fluoride), the supernatant was loaded onto a phosphocellulose P-11 column (Whatman) pre-cycled with 0.5 M NaOH and then equilibrated with extraction buffer A. Recombinant tau bound on the column was eluted with a linear gradient of 0–0.5 M NaCl in extraction buffer A. The pooled fractions containing tau were concentrated with Centrprep centrifugal filter devices (Millipore Corp.) and dialyzed against extraction buffer A. After determination by Coomassie protein assay reagent (Pierce) using bovine serum albumin as the standard, tau was stored frozen at –80 °C until used.

**Plasmid and DNA Constructs of Human Recombinant p35-CDK5 and p25-CDK5 Complexes**—The cDNA for human CDK5 in pCMV was excised with *Bam*HI and ligated into the *Bam*HI site of a baculovirus

\* The costs of publication of this article were defrayed in part by the payment of page charges. This article must therefore be hereby marked "advertisement" in accordance with 18 U.S.C. Section 1734 solely to indicate this fact.

§ To whom correspondence should be addressed. Tel.: 81-3-3351-6141 (ext. 279/248); Fax: 81-3-5379-0658; E-mail: Mhashigu@aol.com.

<sup>1</sup> The abbreviations used are: PHF, paired helical filament; CDK5, cyclin-dependent kinase-5; PIPES, 1,4-piperazinediethanesulfonic acid; MOPS, 4-morpholinepropanesulfonic acid.

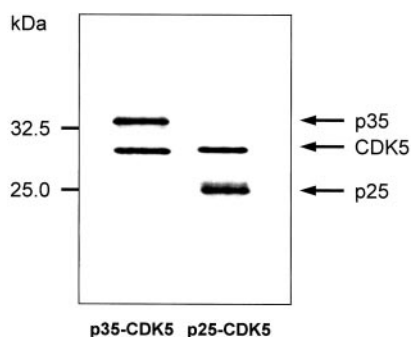


**FIG. 1. Western blot analysis of human recombinant p35-CDK5 and p25-CDK5 complexes.** His<sub>6</sub>-tagged recombinant p35-CDK5 and p25-CDK5 complexes were obtained from coexpression of CDK5 with either p35-His<sub>6</sub> or p25-His<sub>6</sub>, respectively, in Sf9 cells. p35-CDK5 and p25-CDK5 complexes purified on a nickel-nitrilotriacetic acid-agarose column were separated by SDS-PAGE and doubly immunoblotted with an anti-p35/p25 antibody (C-19) and an anti-CDK5 antibody (C-8). Each component of the CDK5 complex clearly cross-reacted with both antibodies, and no impurity was detected.

transfer vector, BacPAK9 (Clontech, Palo Alto, CA). C-terminally His<sub>6</sub>-tagged p35 was generated by PCR amplification using pET23a-p35 as the template and oligonucleotides 5'-GGCGAATTCATGGGCACGGT-GCTGTCCCT-3' and 5'-GGGCTTTAGCGGCCGCCGATCTCAGTG-3' as the primers. The PCR product was cleaved with *Eco*RI and *Not*I and ligated into BacPAK9. His<sub>6</sub>-tagged p25, a deletion of amino acids 1–98 of His<sub>6</sub>-tagged p35 in BacPAK9, was generated by PCR-based mutagenesis. BacPAK9 containing CDK5, p35, or p25 cDNA was cotransfected with BacPAK6 virus DNA (Clontech) into Sf9 cells following the manufacturer's instructions.

**Purification of Human Recombinant p35-CDK5 and p25-CDK5 Complexes**—Human CDK5 stock virus was coexpressed with either p35-His<sub>6</sub> or p25-His<sub>6</sub> virus in Sf9 cells. The Sf9 cell-expressed human recombinant CDK5 complexes were harvested with cold phosphate-buffered saline and centrifuged at 1600 × *g* for 3 min at 4 °C, and the pellet was frozen in liquid nitrogen. The frozen pellet was thawed at 30 °C, resuspended in cold extraction buffer B (10 mM Tris-HCl, pH 8.0, 0.5 M NaCl, 1% Triton X-100, 10 mM imidazole, 10 mM β-mercaptoethanol, 0.2 mM Pefabloc SC, 1 μM E-64, and 10 μg/ml leupeptin), and sonicated three times for 10 s each at 4 °C. The cell suspension was centrifuged at 19,000 × *g* for 15 min at 4 °C. The supernatant was transferred onto a nickel-nitrilotriacetic acid-agarose column that was prewashed with extraction buffer B and then with wash buffer (10 mM Tris-HCl, pH 7.5, 0.15 M NaCl, and 5 mM imidazole) at 4 °C. The p35-CDK5 or p25-CDK5 complex bound on the column was eluted with 10 mM Tris-HCl, pH 7.5, 0.15 M NaCl, and 350 mM imidazole. The pooled fractions containing p35-CDK5 or p25-CDK5 were dialyzed against dialysis buffer (10 mM MOPS, pH 6.8, 5 mM MgCl<sub>2</sub>, 1 mM dithiothreitol, 100 mM KCl, and 10% glycerol). The concentrations of recombinant CDK5 complexes were determined using the Coomassie protein assay kit (Pierce) with bovine serum albumin as the standard. The purity of the purified human recombinant p35-CDK5 and p25-CDK5 complexes was assessed by double immunostaining with an anti-p35/p25 polyclonal antibody (C-19; Santa Cruz Biotechnology, Santa Cruz, CA) and an anti-CDK5 polyclonal antibody (C-8; Santa Cruz Biotechnology) at 1:1000 and 1:2000 dilutions, respectively (Fig. 1).

**In Vitro Kinetic Analysis of Tau Phosphorylation**—The kinase activities of the p35-CDK5 and p25-CDK5 complexes were determined as described (14), except that the p35-CDK5 and p25-CDK5 complexes were used at a concentration of 15 μg/ml with recombinant tau or histone H1. The kinase assay was initiated by adding the p35-CDK5 or p25-CDK5 complex to the reaction mixtures, and then an aliquot of the reaction mixture was withdrawn and placed into a new tube containing SDS sample buffer to terminate the reaction after various incubation times. The assay mixtures were separated by SDS-PAGE, and the bands containing phosphorylated substrate were excised from the gel. For the time course analysis, <sup>32</sup>P<sub>i</sub> incorporation into tau or histone H1 was quantified by Cerenkov counting using a liquid scintillation analyzer (PerkinElmer Life Sciences). The tau bands were also saved for phosphopeptide mapping. A control reaction was performed with the same assay mixture containing bovine serum albumin instead of tau or histone H1.

**Phosphorylation after Occlusion of Phosphorylatable Sites by p35-CDK5 or p25-CDK5 Preincubation**—Tau (0.25 mg/ml) was preincubated with the p35-CDK5 or p25-CDK5 complex (15 μg/ml) and 1 mM

unlabeled ATP for 23 h at 30 °C. For additional phosphorylation after occlusion by the first CDK5 complex, two separate aliquots (20 μl) from preincubation mixtures were transferred to new tubes and then incubated with fresh p35-CDK5 or p25-CDK5 complex (15 μg/ml), MgCl<sub>2</sub> (10 mM), dithiothreitol (0.2 mM), and [γ-<sup>32</sup>P]ATP (1 mM) for another 4.5 h at 30 °C. The reactions were stopped by adding SDS-PAGE sample buffer to the assay mixtures and analyzed by tryptic phosphopeptide mapping.

**Tryptic Phosphopeptide Mapping of Recombinant Tau**—Recombinant tau was phosphorylated by the p35-CDK5 or p25-CDK5 complex for a particular time period at 30 °C, and then phosphorylated tau was separated by SDS-PAGE (see "In Vitro Kinetic Analysis of Tau Phosphorylation"). The bands containing tau were excised from the gel, washed three times with 25% isopropyl alcohol for 30 min, and then washed overnight with 10% methanol at room temperature. The tau bands were dried overnight at 50 °C and digested with 50 μg/ml trypsin (L-1-tosylamido-2-phenylethyl chloromethyl ketone-treated trypsin; Sigma) in 50 mM NH<sub>4</sub>HCO<sub>3</sub>, pH 8.4, overnight at 30 °C. The digested peptide extract was transferred to a new tube and dried with a vacuum evaporator. Dried peptides were washed with 100 μl of doubly distilled water. After centrifugal concentration, the radioactivity of the dried peptide was quantified by Cerenkov counting. The digested phosphopeptide was dissolved in TLC buffer (formic acid (88%)/glacial acetic acid/water (50:150:800), pH 1.9). An aliquot of the digested phosphopeptides containing ~1000 cpm of radioactivity/plate was subjected to phosphopeptide mapping using silica gel thin-layer plates (Merck, Darmstadt, Germany). The first dimension of electrophoresis was carried out in TLC buffer, pH 1.9, at 10 °C; the second dimension of chromatography was carried out in *n*-butyl alcohol/pyridine/glacial acetic acid/water (150:100:30:120). The plates were analyzed with a BAS 2000II bioimaging analyzer (Fuji Film, Tokyo, Japan). The silica gel on the separated phosphopeptide spots (spots 1–5) was then scratched off of the plates and recovered in scintillation vials. The radioactivity of each spot was quantified by Cerenkov counting.

**Antibodies**—An anti-tau monoclonal antibody (Tau-1) was purchased from Roche Molecular Biochemicals, and an anti-phospho-Ser<sup>202</sup> tau antibody (referred to below as the pS202 antibody) was obtained from Sigma. Tau-5 was purchased from NeoMarkers. A phosphorylation-dependent anti-tau antibody (AT8) was obtained from Santa Cruz Biotechnology.

**Western Blot Analysis**—Kinase assays were carried out as described (14). Phosphorylated tau was separated by SDS-PAGE and transferred to polyvinylidene difluoride membranes. The blotted membrane was immunostained with one of the anti-tau antibodies and then stripped with stripping buffer (62.5 mM Tris-HCl, pH 6.7, 100 mM 2-mercaptoethanol, and 2% SDS) for 30 min at 50 °C. The membrane was reprobed with a different anti-tau antibody. We used anti-tau antibody AT8, the pS202 antibody, and Tau-1 at 1:500, 1:2000, and 0.5 μg/ml dilutions, respectively. The total immunoreactivity of tau against Tau-5 (1 μg/ml) was routinely monitored to adjust the total amount of loaded samples (data not shown).

**Statistics**—All data were analyzed by analysis of variance (SYSTAT Version 4, SYSTAT, Evanston, IL), and values were considered significantly different when *p* < 0.05.

## RESULTS

**Time Course of Phosphorylation of and P<sub>i</sub> Incorporation into Tau**—A low concentration (less than one-tenth of the *K<sub>m</sub>*) of recombinant tau (0.2 mg/ml) was incubated in the kinase assay mixture with the p25-CDK5 or p35-CDK5 complex. Aliquots of the assay mixture were withdrawn at 15, 30, 60, 120, 300, and 480 min. After separation of tau by SDS-PAGE, <sup>32</sup>P<sub>i</sub> incorporation into tau was measured using a scintillation counter. A typical result is illustrated in Fig. 2. Incorporation of P<sub>i</sub> into tau by the p35-CDK5 complex was found to be very slow. In contrast, the rate of P<sub>i</sub> incorporation into tau was much faster when it was incubated with the p25-CDK5 complex.

Assuming a single exponential reaction, the time constant of the overall phosphorylation process could be determined. In the example depicted in Fig. 2, the time constants of P<sub>i</sub> incorporation by p35-CDK5 and p25-CDK5 complexes were 164 and 68 min, respectively. Thus, phosphorylation by the p35-CDK5 complex was 2.4 times slower than that by the p25-CDK5 complex. No phosphorylation of bovine serum albumin was seen upon incubation with the CDK5 complexes (data not shown).

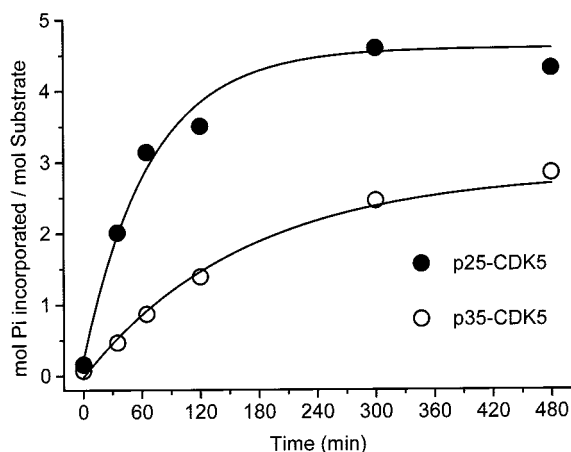


FIG. 2. Time course of phosphorylation of tau by the p35-CDK5 and p25-CDK5 complexes. Recombinant tau was incubated with the p35-CDK5 or p25-CDK5 complex at 30 °C, and an aliquot of the reaction mixture was withdrawn. Phosphorylation of tau was analyzed by excising tau bands from SDS gels and counting the radioactivity of the gels with a scintillation counter. A line was drawn assuming a single exponential reaction.

**Stoichiometry of  $P_i$  Incorporation into Tau**—Upon saturation of  $P_i$  incorporation, we found that 3.3 and 2.3 mol of  $P_i$  were incorporated into 1 mol of tau by the p25-CDK5 and p35-CDK5 complexes, respectively (Table I). Thus, the p25-CDK5 complex could phosphorylate at least three different sites of tau. In contrast, at least two sites could be phosphorylated by the p35-CDK5 complex. The results from four separate experiments are tabulated in Table I.

**Apparent Kinetic Parameters of Overall Phosphorylation of Tau**—Although tau possesses multiple sites of phosphorylation, overall  $P_i$  incorporation by CDK5 was found to be described by the Michaelis-Menten equation. The apparent kinetic parameters  $K_m$  and  $k_{cat}$  (or turnover number) were determined.

Considering the temporal characteristics, the initial velocity of phosphorylation of tau by  $P_i$  incorporation with the p35-CDK5 or p25-CDK5 complex was determined after a 35- and 15-min reaction period, respectively. Whenever possible, the initial velocity was determined using exponential fitting of data obtained during different reaction periods. Values obtained by both methods agreed reasonably well.

The velocity of phosphorylation (expressed as moles of  $P_i$ /mol of enzyme/min) was determined from  $^{32}P_i$  incorporation at three different substrate concentrations. The results were analyzed in a Hanes-Woolf plot (Table II). The Michaelis constant ( $K_m$ ) for phosphorylation of tau by the CDK5 complex was almost the same with either p35 or p25 (Table II), indicating that the apparent affinity of tau for the CDK5 complex was not modified by the regulatory units of CDK5.

Interestingly, the  $k_{cat}$  (turnover number) for tau phosphorylation by p25-CDK5 was significantly greater than that by p35-CDK5 ( $p < 0.05$ ) (Table II). Judging from the  $k_{cat}/K_m$  value, an indicator of enzyme potency, the p25-CDK5 complex was found to be ~6 times more rapid in incorporating  $P_i$  into tau.

The cooperativity of overall phosphorylation of tau by a CDK5 complex was examined using a Hill plot. The Hill numbers of the reaction with the p35-CDK5 and p25-CDK5 complexes were  $0.75 \pm 0.3$  and  $1.1 \pm 0.4$  (mean  $\pm$  S.D.,  $n = 3$ ), respectively. These values mean no or little cooperativity, and the difference between them was not significant.

**Time Course and Kinetic Parameters of Histone H1 Phosphorylation**—Similarly, the phosphorylation of histone H1, a frequently employed but non-physiologic substrate, was studied

as well (data not shown). The time constants of  $P_i$  incorporation by p35-CDK5 and by p25-CDK5 were  $69 \pm 10$  and  $16 \pm 3.8$  min, respectively. Phosphorylation of histone H1 by the p35-CDK5 complex was indeed slower than that by the p25-CDK5 complex. The kinetic parameters of CDK5-induced histone H1 phosphorylation were determined (Table II).

**Tryptic Phosphopeptide Maps of Tau Phosphorylated by CDK5 Complexes**—To investigate the characteristics of CDK5-induced phosphorylation of each serine or threonine residue of tau, phosphopeptide mapping of tryptic digests was conducted. Both unsaturated and saturated stages of phosphorylation were subjected to analysis.

Considering the fact that the p25-CDK5 complex incorporated  $P_i$  into tau twice as fast as the p35-CDK5 complex, kinase action was terminated after 0.5 and 1 h for the p25-CDK5 and p35-CDK5 complexes, respectively. The duration was chosen to be approximately half of the time constant of each CDK5 complex so that 63% of the phosphorylatable sites were phosphorylated in each case. An extended reaction time of 8 or 23 h was adapted to saturate all of the phosphorylatable sites. A typical example of phosphopeptide mapping is shown in Fig. 3. The maps reveal five major spots and some minor spots after 8 h of phosphorylation (Fig. 3, C and D).

In contrast to the density of the other spots, the density of spot 1 obtained after 1 h of reaction was weak in the presence of either p35 or p25 (Fig. 3, A and B), indicating that spot 1 was phosphorylated more slowly than the other spots. In fact, the density of spot 1 obtained after 8 h of reaction with the p25-CDK5 complex was comparable with those of the other spots (Fig. 3D). However, the density of spot 1 obtained after 8 h of reaction with the p35-CDK5 complex was still weaker (Fig. 3C).

**Identification of the Peptide Sequence Corresponding to Each of the Major Spots**—The predicted locations of the peptides known to be phosphorylated by CDK5 complexes were calculated by the method described by Boyle *et al.* (15). A comparison between the observed and predicted phosphopeptide maps revealed that spot 1 corresponded to the doubly phosphorylated Ser<sup>202</sup>/Thr<sup>205</sup> peptide (<sup>195</sup>SGYSSPGSPGTPGSR<sup>209</sup>). Spots 2 and 3 corresponded to the phosphorylated Ser<sup>202</sup> peptide (<sup>195</sup>SGYSSPGSPGTPGSR<sup>209</sup>) and the phosphorylated Ser<sup>404</sup> peptide (<sup>396</sup>SPVVS GDTSPR<sup>406</sup>), respectively. Spots 4 and 5 seemed to be derived from fully and partially digested Ser<sup>235</sup> peptides (<sup>231</sup>TPPKSPSSAK<sup>240</sup> and <sup>235</sup>SPSSAK<sup>240</sup>, respectively).

**Time-dependence of  $P_i$  Incorporation into Spots**—To quantify the time-dependent phosphorylation of the five major spots,  $^{32}P_i$  incorporation into each spot was measured. After visualization of the spots using the BAS 2000II bioimaging analyzer, each spot was marked. The silica gel on each spot was then removed from the glass plate, and radioactivity was measured using a scintillation counter (see "Experimental Procedures").

Fig. 4 illustrates a typical example of such experiments. Only spot 1 was plotted. After 8 h of incubation, the p25-CDK5 complex was found to phosphorylate Ser<sup>202</sup>/Thr<sup>205</sup> (corresponding to spot 1) to a steady level. In contrast, phosphorylation of Ser<sup>202</sup>/Thr<sup>205</sup> by the p35-CDK5 complex was extremely slow compared with the other sites. Even after 8 h of incubation, the density of spot 1 remained <5% of the sum of  $P_i$  incorporation into the five major spots.

The phosphorylation rate of Ser<sup>202</sup> (corresponding to spot 2) alone was found to be much faster than the double phosphorylation of Ser<sup>202</sup>/Thr<sup>205</sup> (Fig. 3). The p35-CDK5 complex increased relative  $^{32}P_i$  incorporation into Ser<sup>202</sup> steadily, whereas a slow decline in relative  $^{32}P_i$  incorporation into Ser<sup>202</sup> was noticed after 2 h. These results indicate that the phosphorylation rate of Ser<sup>202</sup> or Thr<sup>205</sup> is slow compared with the



TABLE I  
Time constants and stoichiometry of phosphorylation of tau and histone H1 by p35-CDK5 or p25-CDK5

Each value was obtained from at least four separate experiments (mean  $\pm$  S.D.).

	Tau		Histone H1	
	Time constant	mol P <sub>i</sub> /substrate	Time constant	mol P <sub>i</sub> /substrate
	min		min	
p35-CDK5	127 $\pm$ 35	2.3 $\pm$ 0.6	69 $\pm$ 10	2.2 $\pm$ 0.6
p25-CDK5	63 $\pm$ 5.5 <sup>a</sup>	3.3 $\pm$ 1.0 <sup>a</sup>	16 $\pm$ 3.8 <sup>a</sup>	2.3 $\pm$ 0.5

<sup>a</sup>  $p < 0.05$ .

TABLE II  
Kinetic parameters of phosphorylation of tau and histone H1 by p35-CDK5 or p25-CDK5

Each value was obtained from five separate experiments (mean  $\pm$  S.D.).

	Tau			Histone H1		
	$K_m$	$k_{cat}$	$k_{cat}/K_m$	$K_m$	$k_{cat}$	$k_{cat}/K_m$
	$\mu M$	$min^{-1}$		$\mu M$	$min^{-1}$	
p35-CDK5	33 $\pm$ 30	2.6 $\pm$ 0.7	0.079	60 $\pm$ 17	14 $\pm$ 10	0.23
p25-CDK5	27 $\pm$ 21	13 $\pm$ 4.5 <sup>a</sup>	0.48	104 $\pm$ 55	81 $\pm$ 74 <sup>a</sup>	0.78

<sup>a</sup>  $p < 0.05$ .

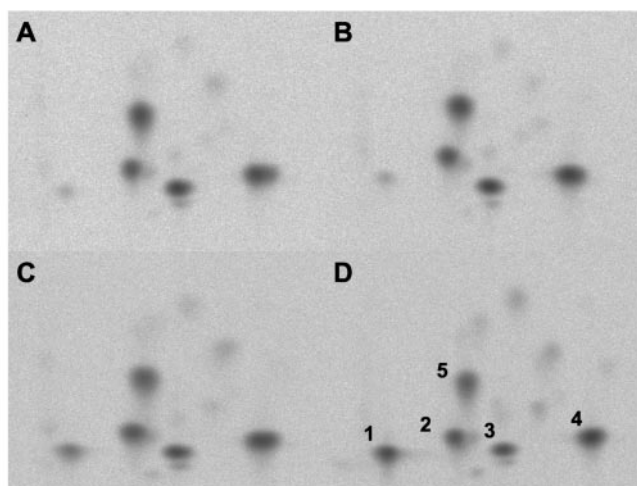


FIG. 3. Tryptic phosphopeptide map of tau phosphorylated by the p35-CDK5 and p25-CDK5 complexes. Recombinant tau was incubated in the reaction mixture containing either the p35-CDK5 complex (A and C) or the p25-CDK5 complex (B and D) at 30 °C. Aliquots of the reaction mixture were withdrawn after 0.5 h (B), 1 h (A), or 8 h (C and D) and subjected to analysis (see "Experimental Procedures"). Five major spots (spots 1–5) and several minor spots were recognized. Note that the p25-CDK5 complex increased remarkably the density of spot 1 after 8 h (D).

overall phosphorylation rate. Furthermore, double phosphorylation of two adjacent sites may be a complicated phenomenon (see below).

**Phosphopeptide Mapping after Occlusion of Phosphorylatable Sites of Tau**—To characterize the slow P<sub>i</sub> incorporation into tau by the CDK5 complex, we carried out phosphopeptide mapping after prolonged incubation with unlabeled ATP. In the experiment depicted in Fig. 5, tau was phosphorylated with unlabeled ATP for 23 h, a period long enough to allow occlusion of most of the phosphorylatable sites of tau; and then [ $\gamma$ -<sup>32</sup>P]ATP was added (see "Experimental Procedures"). Thus, P<sub>i</sub> incorporation into tau after occlusion was readily visualized by phosphopeptide mapping (Fig. 5).

After an extended incubation of tau with the p25-CDK5 complex, addition of [ $\gamma$ -<sup>32</sup>P]ATP with fresh p25-CDK5 complex resulted in a remarkable increase in the density of spot 1. The rest of the spots became only faintly noticeable (Fig. 5, Top). Thus, double phosphorylation of Ser<sup>202</sup> and Thr<sup>205</sup> (spot 1) was not accomplished by the p25-CDK5 complex, whereas single phosphorylation of Ser<sup>202</sup> (spot 2) was almost complete. In

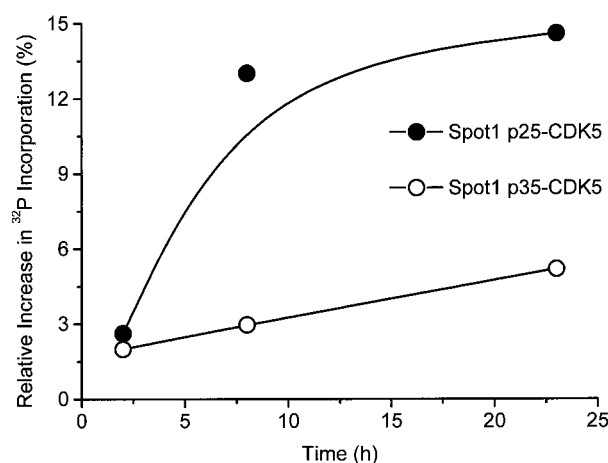


FIG. 4. Time course of P<sub>i</sub> incorporation into spot 1. Relative <sup>32</sup>P<sub>i</sub> incorporation into spot 1 was measured at 2, 8, and 23 h and plotted. Note that the radioactivity of spot 1 is expressed as a fraction of the total radioactivity of the five major spots.

contrast, addition of the p35-CDK5 complex after occlusion by the p25-CDK5 complex failed to increase the density of specific sites (data not shown).

Tau was also incubated with the p35-CDK5 complex for 23 h with unlabeled ATP. P<sub>i</sub> incorporation was then visualized by addition of [ $\gamma$ -<sup>32</sup>P]ATP together with the p25-CDK5 complex. In this case, both spots 1 and 2 became dense (Fig. 5, Bottom), suggesting that neither Ser<sup>202</sup> nor Thr<sup>205</sup> was occluded by the p35-CDK5 complex.

**Western Blot Analysis of Tau Using Phosphorylation-dependent Anti-tau Antibodies**—Site-specific phosphorylation of tau was analyzed using phosphorylation-dependent anti-tau antibodies over an extended period of up to 24 h. Aliquots were withdrawn from the reaction mixture, and proteins were separated by SDS-PAGE. The proteins were transferred to a membrane that was then probed with anti-tau antibody. Whenever possible, the membrane was stripped and reprobed with other anti-tau antibodies.

AT8 reactivity was first detected 3 h after incubation with the p25-CDK5 complex. It developed slowly during the subsequent incubation period. After 24 h of incubation, prominent AT8 reactivity was achieved by the p25-CDK5 complex. In contrast, only a faint AT8 signal was detected with the p35-CDK5 complex even after 24 h of incubation (Fig. 6A). The p25-CDK5 complex had a much higher level of phosphorylation on the AT8 epitopes compared with the p35-CDK5 complex.

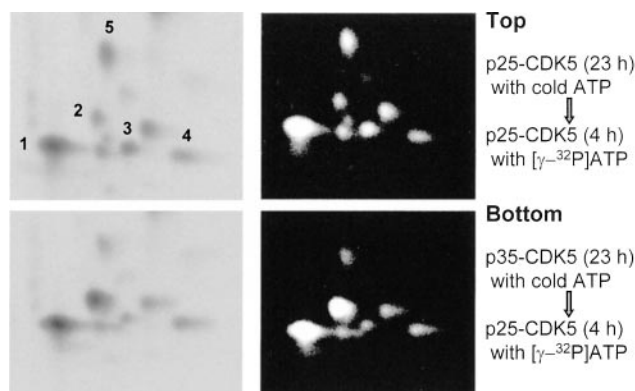


FIG. 5. **Phosphopeptide map of phosphorylated tau after occlusion of phosphorylatable sites.** Recombinant tau was phosphorylated by the CDK5 complexes with unlabeled ATP for 23 h, a period long enough to allow occlusion of most of the phosphorylatable sites; and then  $[\gamma\text{-}^{32}\text{P}]$  ATP was added to an aliquot of the p35-CDK5 (Bottom) or p25-CDK5 (Top) preincubation mixture together with fresh CDK5 complex. After an additional incubation period, aliquots were withdrawn and subjected to analysis. Autoradiographs with the BAS 2000II Bioimage analyzer (left panels) and their enhanced images (right panels) are shown. Top, after occlusion by the p25-CDK5 complex, addition of fresh p25-CDK5 complex induced  $^{32}\text{P}_i$  incorporation into spot 1; Bottom, after occlusion by the p35-CDK5 complex, fresh p25-CDK5 complex induced  $^{32}\text{P}_i$  incorporation into spots 1 and 2.

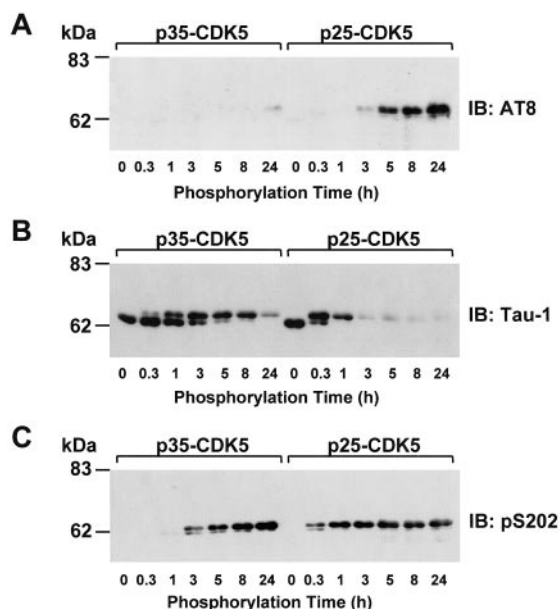


FIG. 6. **Immunoblot analysis of site-specific phosphorylation of tau catalyzed by the p35-CDK5 or p25-CDK5 complex.** Tau was phosphorylated by the p35-CDK5 or p25-CDK5 complex. Aliquots of the mixtures were withdrawn at the indicated times and immunoblotted (IB) with phosphorylation-dependent anti-tau antibody AT8 (A), the pS202 antibody (C), and dephosphorylation-dependent anti-tau antibody Tau-1 (B). Each analysis used the same membrane, which was stripped. Similar results were obtained in three separate experiments.

Phosphorylation of Ser<sup>202</sup>/Thr<sup>205</sup> was also monitored by Tau-1 using the same membrane. After 20 min of incubation with the p25-CDK5 complex, the Tau-1 band showed a retardation in mobility, and then the Tau-1 signal began to disappear progressively. The Tau-1 signal became negligible 1 h after incubation with the p25-CDK5 complex, indicating that unphosphorylated Ser<sup>202</sup> or Thr<sup>205</sup> diminished steadily. The change in Tau-1 reactivity after incubation with p35-CDK5 was essentially the same as for the p25-CDK5 complex, but was very slow; the mobility of the Tau-1 band began to retard, and then Tau-1 reactivity disappeared progressively (Fig. 6B).

The same membrane was reprobed with the pS202 antibody, an anti-tau antibody raised solely against phosphorylated Ser<sup>202</sup>. When tau was phosphorylated by the p35-CDK5 complex, the pS202 antibody signal became detectable after 3 h of incubation, with an indication of a retardation in mobility, and then it became dense very slowly, without any indication of saturation, even after 24 h. As expected, the p25-CDK5 complex induced a rapid increase in the reactivity of the pS202 antibody, maximizing during the 3-h incubation period (Fig. 6C).

As phosphorylation proceeded, the mobility of the pS202 antibody band became retarded. However, a decrease in the reactivity of the pS202 antibody after prolonged exposure to the p25-CDK5 complex was not associated with a mobility change. Thus, the observed decrease in the pS202 antibody reactivity did not result from dephosphorylation of the pS202 antibody.

## DISCUSSION

This study determined the kinetic characteristics of *in vitro* phosphorylation of tau by CDK5 complexes using recombinant proteins. The p25-CDK5 complex was found to phosphorylate tau much faster than the p35-CDK5 complex. On the assumption that the time course of total phosphorylation can be approximated by a single exponential reaction, the time constant of the decline in phosphorylatable sites was determined, and the results suggest that p25 can accelerate the catalytic activity of CDK5 by  $\sim 2.4$ -fold compared with p35.

We determined the stoichiometry (moles of  $\text{P}_i$ /mol of tau) of tau phosphorylation by CDK5 and found that the p25-CDK5 complex can phosphorylate tau faster. Furthermore, it can incorporate more phosphate into tau compared with the p35-CDK5 complex.

The stoichiometry of tau phosphorylation by neuronal cdc2-like protein kinase (brain-derived p25-CDK5 complex) was reported to be 3.8 mol of phosphate/mol of tau (5). Thus, the recombinant p25-CDK5 complex used in the present study is as potent as the naturally occurring CDK5 complex. Sironi *et al.* (16) studied *in vitro* phosphorylation of tau at Ser<sup>262</sup> by three different kinases (calcium/calmodulin-dependent protein kinase II, protein kinase A, and phosphorylase kinase) and found that total  $\text{P}_i$  incorporation into tau by any of the three enzymes saturated after 100 min of reaction. Upon saturation of overall phosphorylation, calcium/calmodulin-dependent protein kinase II, protein kinase A, and phosphorylase kinase incorporated 0.9–1.2 mol of phosphate/mol of tau. Purified phosphorylase kinase from rabbit skeletal muscle reportedly phosphorylated tau to a stoichiometry of 2.1 mol of phosphate/mol of tau (17). Compared with these results, the stoichiometry of overall phosphorylation of tau by the p25-CDK5 complex is characteristically high. To evaluate the phosphorylation of tau by CDK5 quantitatively, kinetic parameters were determined using the Michaelis-Menten equation. The apparent  $K_m$  and  $k_{\text{cat}}$  values for tau phosphorylation by the p35-CDK5 complex were 33  $\mu\text{M}$  and 2.6  $\text{min}^{-1}$ , respectively. The  $K_m$  value for the p25-CDK5 complex was 27  $\mu\text{M}$  and was unchanged from that for the p35-CDK5 complex ( $p < 0.05$ ,  $n = 4$ ). The  $k_{\text{cat}}$  value for the p25-CDK5 complex was 13  $\text{min}^{-1}$  and was significantly larger than that for the p35-CDK5 ( $p < 0.05$ ,  $n = 4$ ). The  $k_{\text{cat}}/K_m$  value for the p25-CDK5 complex was 6 times larger than that for the p35-CDK5 complex.

The kinetic parameters of CDK5 complexes were also determined using histone H1 as a substrate. The observed  $K_m$  value for the p35-CDK5 complex was in good agreement with previous results (18). The difference in the  $K_m$  values for the p25-CDK5 and p35-CDK5 complexes was not significant, whereas the  $k_{\text{cat}}/K_m$  value for the p25-CDK5 complex was significantly larger than that for the p35-CDK5 complex. Thus, the p25-CDK5 complex is a much more potent kinase, and the p25

regulatory unit accelerates the reactivity of CDK5 without changing its affinity for tau.

For tau phosphorylation by phosphorylase kinase, the  $K_m$  and  $k_{cat}$  values were 6.9  $\mu M$  and 47.4  $\text{min}^{-1}$ , respectively, indicating that phosphorylase kinase has a better affinity for tau and more efficient turnover of catalytic activity compared with CDK5 complexes (17). But the stoichiometry of total phosphorylation of tau by the p25-CDK5 complex is larger than that for the other tau kinases, including the p35-CDK5 complex. As a tau kinase, p25-CDK5 could contribute to the high phosphorylation stoichiometry of PHF-tau.

Our analysis of the total phosphorylation of tau revealed a difference in the catalytic activity of CDK5 complexes; site-specific phosphorylation must be clarified for a better understanding of CDK5. We have employed two independent approaches: phosphopeptide mapping of the tryptic digest of tau and Western blot analysis with phosphorylation-dependent anti-tau antibodies.

By comparing the phosphopeptide maps for the early and saturated stages of phosphorylation, we found that  $^{32}\text{P}_i$  incorporation into spot 1 was very slow. In contrast,  $^{32}\text{P}_i$  incorporation into the other four spots was almost complete within 120 min, suggesting that the time course of overall phosphorylation of tau depends on the phosphorylation kinetics of Ser<sup>202</sup>, Ser<sup>235</sup>, and Ser<sup>404</sup>. We further examined this unreported characteristic of site-specific phosphorylation of Ser<sup>202</sup> and Thr<sup>205</sup>.

We have made the following observations. (a) The p35-CDK5 complex promoted  $^{32}\text{P}_i$  incorporation into spot 1 very slowly; and (b) the p25-CDK5 complex promoted  $^{32}\text{P}_i$  incorporation into spot 1 more rapidly, but only after 2 h. These results raise the possibility of sequential phosphorylation of Thr<sup>205</sup> after Ser<sup>202</sup>.

To investigate  $^{32}\text{P}_i$  incorporation, we conducted phosphopeptide mapping after having occluded possible phosphorylation sites with unlabeled ATP. Newly incorporated  $^{32}\text{P}_i$  was visualized as an intense spot on the map. After occlusion with the p25-CDK5 complex, p25-CDK5 promoted  $^{32}\text{P}_i$  incorporation into spot 1 only.  $^{32}\text{P}_i$  incorporation into any of the major spots did not happen. These findings suggest that phosphorylation of Ser<sup>202</sup> was already saturated and that only Thr<sup>205</sup> was slowly phosphorylated over the extended time of incubation. In contrast, the p35-CDK5 complex failed to occlude both spots 1 and 2, as suggested by the intense signal on the two spots. The occlusion experiment also confirmed that slow phosphorylation by CDK5 complexes happens only at Ser<sup>202</sup> and Thr<sup>205</sup>.

To clarify further the time dependence of phosphorylation of Ser<sup>202</sup> and Thr<sup>205</sup>, Western blot analysis of tau was carried out. The three phosphorylation-dependent anti-tau antibodies have distinct epitopes. AT8 reacts with tau only when multiple sites around Ser<sup>202</sup>, including Ser<sup>199</sup>, Ser<sup>202</sup>, and Thr<sup>205</sup>, are phosphorylated. Single phosphorylation of any of the residues is not enough for AT8 reactivity (19, 20). Thus, AT8 is useful in detecting phosphorylation of Ser<sup>202</sup>/Thr<sup>205</sup> for proline-directed kinases, including CDK5 complexes. In contrast, Tau-1 requires an absolutely non-phosphorylated epitope around Ser<sup>202</sup> (21). In the present study, Tau-1 reacted with recombinant tau quite well. However, phosphorylation of Ser<sup>202</sup> or Thr<sup>205</sup> caused loss of Tau-1 reactivity. The pS202 antibody is raised against phosphorylated Ser<sup>202</sup> of human tau.

AT8 reactivity was latent, whereas the Tau-1 signal started to decline without delay, suggesting that Ser<sup>202</sup> and Thr<sup>205</sup> cannot be phosphorylated simultaneously. Either Ser<sup>202</sup> or Thr<sup>205</sup> must be phosphorylated first. The phosphorylated Ser<sup>202</sup> signal (immunoreactivity of the pS202 antibody) started to develop as soon as the Tau-1 signal disappeared. Although phosphorylation of Thr<sup>205</sup> as a first step of sequential phospho-

rylation cannot be ruled out, the initial phosphorylation of Ser<sup>202</sup> and the subsequent phosphorylation of Thr<sup>205</sup> seem to be the principal route to double phosphorylation.

Many of the pathologic epitopes on hyperphosphorylated tau in the brains of Alzheimer's disease patients were thought to be generated by sequential phosphorylation by different tau kinases. For example, phosphorylation of a specific amino acid residue by CDK5 is a prerequisite for the subsequent kinase action of glycogen synthase kinase-3 $\beta$  (22, 23). Phosphorylation of Thr<sup>212</sup> by glycogen synthase kinase-3 $\beta$  is known to facilitate protein kinase A action on Ser<sup>214</sup> (4). Such hierarchy among tau kinases (24) makes it complicated to clarify the mechanism of abnormal phosphorylation of tau.

We have shown evidence for the sequential phosphorylation of Ser<sup>202</sup> and Thr<sup>205</sup> of tau by the p25-CDK5 complex. Phosphorylation of Thr<sup>205</sup> occurred only after Ser<sup>202</sup> was phosphorylated. As a result, phosphorylation of Thr<sup>205</sup> was extremely slow compared with phosphorylation of other sites such as Ser<sup>235</sup> and Ser<sup>404</sup>. In addition, the p35-CDK5 complex had weak or negligible kinase action on Thr<sup>205</sup>.

Our findings strongly suggest that cleavage of p35 to p25 regulates not only the overall kinase activity of CDK5, but also the sequential phosphorylation of Ser<sup>202</sup> and Thr<sup>205</sup>. The association of CDK5 with a particular activator unit, p35 or p25, provides a novel mechanism of controlling kinase characteristics.

**Acknowledgments**—We appreciate the initial help of Dr. H. K. Paudel. We thank Dr. L. H. Tsai for providing human CDK5 cDNA and Dr. M. Goedert for the gift of human tau cDNA.

## REFERENCES

- Lee, V. M., Goedert, M., and Trojanowski, J. Q. (2001) *Annu. Rev. Neurosci.* **24**, 1121–1159
- Luc, B., Thierry, B., Valrie, B. S., Andre, D., and Patrick, R. H. (2000) *Brain Res. Rev.* **33**, 95–130
- Morishima-Kawashima, M., Hasegawa, M., Takio, K., Suzuki, M., Yoshida, H., Titani, K., and Ihara, Y. (1995) *J. Biol. Chem.* **270**, 823–829
- Zheng-Fischhofer, Q., Biernat, J., Mandelkow, E. M., Illenberger, S., Godemann, R., and Mandelkow, E. (1998) *Eur. J. Biochem.* **252**, 542–552
- Paudel, H. K., Lew, J., Ali, Z., and Wang, J. H. (1993) *J. Biol. Chem.* **268**, 23512–23518
- Paudel, H. K. (1997) *J. Biol. Chem.* **272**, 28328–28334
- Maccioni, R. B., Otth, C., Concha, I. I., and Munoz, J. P. (2001) *Eur. J. Biochem.* **268**, 1518–1527
- Patrick, G. N., Zukerberg, L., Nikolic, M., De La Monte, S., Dikkes, P., and Tsai, L. H. (1999) *Nature* **402**, 615–622
- Kusakawa, G., Saito, T., Onuki, R., Ishiguro, K., Kishimoto, T., and Hisanaga, S. (2000) *J. Biol. Chem.* **275**, 17166–17172
- Lee, M. S., Kwon, Y. T., Li, M., Peng, J., Friedlander, R. M., and Tsai, L. H. (2000) *Nature* **405**, 360–364
- Smith, D. S., Greer, P. L., and Tsai, L. H. (2001) *Cell Growth & Differ.* **12**, 277–283
- Taniguchi, S., Fujita, Y., Hayashi, S., Kakita, A., Takahashi, H., Murayama, S., Saido, T. C., Hisanaga, S., Iwatsubo, T., and Hasegawa, M. (2001) *FEBS Lett.* **489**, 46–50
- Sobue, K., Agarwal-Mawal, A., Li, W., Sun, W., Miura, Y., and Paudel, H. K. (2000) *J. Biol. Chem.* **275**, 16673–16680
- Hashiguchi, M., Sobue, K., and Paudel, H. K. (2000) *J. Biol. Chem.* **275**, 25247–25254
- Boyle, W. J., van der Geer, P., and Hunter, T. (1991) *Methods Enzymol.* **201**, 110–149
- Sironi, J. J., Yen, S. H., Gondal, J. A., Wu, Q., Grundke-Iqbal, I., and Iqbal, K. (1998) *FEBS Lett.* **436**, 471–475
- Paudel, H. K. (1997) *J. Biol. Chem.* **272**, 1777–1785
- Sharma, P., Steinbach, P. J., Sharma, M., Amin, N. D., Barchi, J. J. Jr., and Pant, H. C. (1999) *J. Biol. Chem.* **274**, 9600–9606
- Goedert, M., Jakes, R., and Vanmechelen, E. (1995) *Neurosci. Lett.* **189**, 167–169
- Preuss, U., Doring, F., Illenberger, S., and Mandelkow, E. M. (1995) *Mol. Biol. Cell* **6**, 1397–1410
- Szendrei, G. I., Lee, V. M., and Otvos, L., Jr. (1993) *J. Neurosci. Res.* **34**, 243–249
- Sengupta, A., Wu, Q., Grundke-Iqbal, K., and Singh, T. (1997) *Mol. Cell. Biochem.* **167**, 99–105
- Alvarez, A., Toro, R., Cacere, A., and Maccioni, R. B. (1999) *FEBS Lett.* **459**, 421–426
- Jicha, G. A., O'Donnell, A., Weaver, C., Angeletti, R., and Davies, P. (1999) *J. Neurochem.* **72**, 214–224